Program Digest, 2019 IEEE International Ultrasonics Symposium (IUS)
Glasgow, Scotland, October 6-9, 2019

Compact Fast-Switching DC and Resonant RF Drivers for a Dual-Mode Imaging and HIFU 2D CMUT Array

Quintin Stedman[1], Lei Gu[1], Chi-Nan Pai[1,2], Morten Rasmussen[1], Kevin Brenner[1], Bo Ma[1], Arif Sanli Ergun[1,3], Juan Rivas Davila[1] and Butrus Khuri-Yakub[1]

[1]Stanford University, Stanford, USA
[2]University of Sao Paulo, Sao Paulo, Brazil
[3]TOBB University of Economics and Technology, Ankara, Turkey

***Abstract*—We developed previously a 2D CMUT array with capability to both do imaging and generate HIFU for ablation of targeted tissues without collateral damage. This new technology allows a more compact HIFU system, when compared to conventional systems composed of HIFU transducers made of PZT, cooling systems for PZT and additional imaging guidance systems. In this paper we present new dc and RF power electronics that drive our 2D CMUT array. The new electronics are significantly more compact and capable of fast-switching between imaging and HIFU mode.**

***Index Terms*—Resonant amplifier, RF, HIFU, Ultrasound imaging, Ablation, CMUT**

I. Introduction

High Intensity Focus Ultrasound (HIFU) is an FDA-approved procedure for ablating targeted tissue without damaging the surrounding tissue [1]. A conventional HIFU system is composed of a PZT transducer for HIFU, a cooling system for the PZT, and either an MRI system or a separate ultrasound imaging system for guidance. So, the entire system is bulky and expensive. We have developed a 2D capacitive micromachined ultrasonic transducer (CMUT) array with capability to both do imaging and generate HIFU [2], [3]. These advantages, plus the lack of self-heating in CMUTs, enable a much more compact and cost effective system. We have previously demonstrated the dual functionality and switching capability of the 2D CMUT array, but with a relatively slow mode switching time (360 ms for HIFU to imaging) caused by the power electronics of the system [4]. Faster switching between HIFU mode and imaging mode is required to provide the user with a frequently-updated image for guidance and potential image bubbles at the ablation site to monitor treatment progress. [5].

We have developed new RF drivers and switchable DC supplies to drive the 2D CMUT array. The new power electronics are compact and can switch quickly between the voltages required for HIFU mode and those required for imaging mode. The results are presented in this paper.

Cliffdale Technologies and Sao Paulo Research Foundation (FAPESP), grant #2018/00710-1

II. 2D CMUT Array

The 2D CMUT array has 32×32 elements with a 250μm pitch in both directions, and a center frequency of 5 MHz in immersion. A dual-mode application-specific integrated circuit (ASIC), developed to perform the imaging and the HIFU processes, was integrated with the CMUT array using flip-chip bonding technology [2], [3]. The CMUT array and asic can be assembles into a probe using a flexible PCB and 3D printed tip, as shown in Fig. 1.

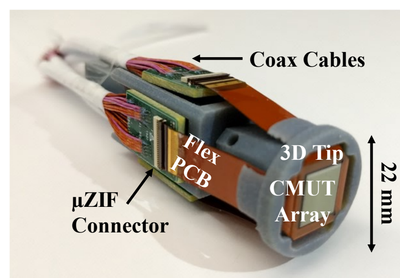

Fig. 1: Assembled HIFU probe with 32×32 2-D CMUT array

The 1024 elements of the CMUT array are divided into 8 groups, as shown in Fig. 2. This gives a fixed focus at 8 mm. 8 channel ac signals with evenly distributed phase among 360° are required to focus the array in HIFU mode. Fig. 3 shows a schematic of operation of the CMUT during HIFU mode, with all 8 channels evenly shifted by 45°.

The CMUT requires a dc bias voltage in addition to the ac driving voltage. Furthermore, the ASIC requires specific dc voltages, which are different in HIFU and imaging mode. We typically drive these CMUT arrays with sine waves in HIFU mode (frequency 5 MHz, amplitude around 60 V_{pp}). Therefore, the developed power electronics consist of two parts: a set of fast-switching dc biasing circuits for the ASIC and CMUT supply voltages, and a compact 8-phase resonant Class-D amplifier for ac signals. The fast switching dc supply circuits use linear regulators with active pulling resistors to drop the voltage from high to low in less than 1 ms.

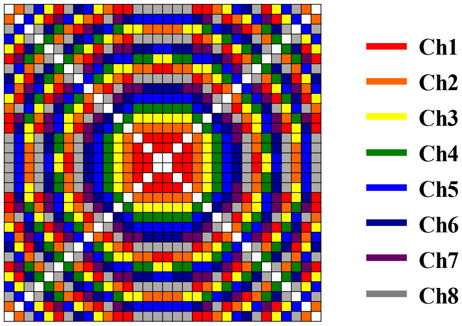

Fig. 2: 2-D CMUT array grouped in 8 channels for focusing

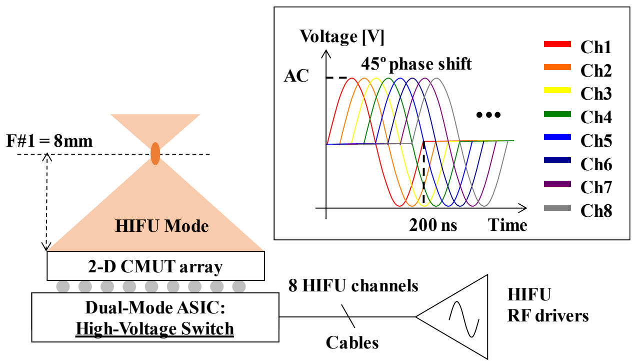

Fig. 3: 8-channel CMUTs are driven by evenly phase-shifted 5 MHz RF signals

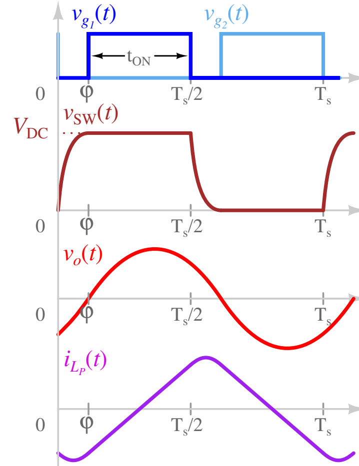

Fig. 5: Typical waveform of the Class-D amplifier in Fig. 4

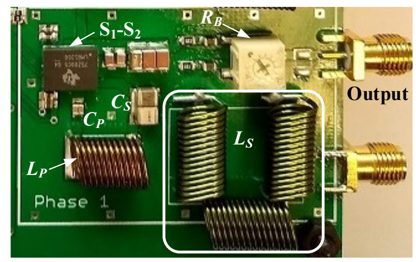

Fig. 6: Prototype picture of a single-channel RF driver

III. 8-Phase 5 MHz Resonant RF Amplifier

To minimize the size and power loss of the RF driver, we selected a half-bridge Class-D resonant amplifier to drive each CMUT channel with a 5 MHz 60 V_{pp} ac signal [6], [7]. The Class-D switch-mode amplifier generates less real power and heat compared with linear amplifier, which reduces the cooling efforts and makes the entire system substantially more compact [4]. Fig. 4, 5, and 6 show a Class-D amplifier's schematic, typical waveform, and the picture of the prototype converter that we designed, respectively.

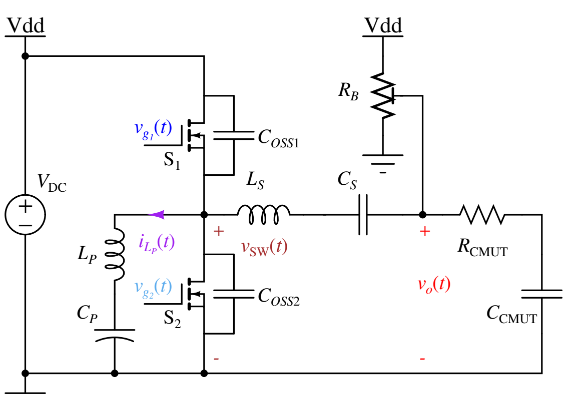

Fig. 4: ZVS Class-D resonant amplifier with parallel inductor

The switched-node voltage $v_{\mathrm{SW}}(t)$ is a 50% square waveform with smooth resonant transition. The two switches $S_{1,2}$ in the circuit achieve zero-voltage switching (ZVS) operation, which eliminates the switching losses and improves the dc-ac conversion efficiency. ZVS operation is achieved through the resonance between the inductor L_P and $S_{1,2}$'s parasitic capacitance $C_{OSS1,2}$ [8]. C_P is a dc block and its voltage is constant as $0.5V_{\mathrm{DC}}$. R_{CMUT} and C_{CMUT} model the effective impedance of each CMUT channel together with all the parasitics from the cable and other electronics at 5 MHz [2]. L_S and C_S form a high-Q series resonant bandpass matching network and only deliver the 5 MHz sine wave voltage signal to the CMUT. As the impedance of L_S and C_S cancel each other, the Peak-to-Peak (PP) output voltage across R_{CMUT}-C_{CMUT} will be $\frac{4}{\pi}V_{\mathrm{DC}}$. R_B is a potentiometer to adjust the output signal's dc level.

The R_{CMUT}-C_{CMUT} values vary slightly among the 8 channels. The average value of R_{CMUT}-C_{CMUT} at 5 MHz is 7.7 Ω-1.67 nF. Table I shows the key components used in the prototype. Using the integrated GaN power stage, LMG5200, significantly simplifies the design and shrinks the driver's size.

We built a RF driver with 8-phase 5 MHz Class-D amplifiers, as shown in Fig. 7. We tested the RF driver with dummy loads, with each channel driving an 1.8 nF capacitor and an 1 Ω resistor. Fig. 8 shows the measured output waveform. The amplitudes of the sine waves reach 60 Vpp. The 8-channel signals are evenly phase shifted by 45°.

TABLE I: Key components of a single-phase Class-D amplifier

Part	Value	Description
$S_{1,2}$	LMG5200	80 V TI Integrated GaN
L_S	1.5 μH	Coilcraft 2929SQ x 3
C_S	675 pF	TDK 500 V C0G
L_P	300 nH	Coilcraft 2929SQ
C_P	0.2 μF	TDK 100 V X7R
R_B	1 kΩ	3361P-1-102GLF

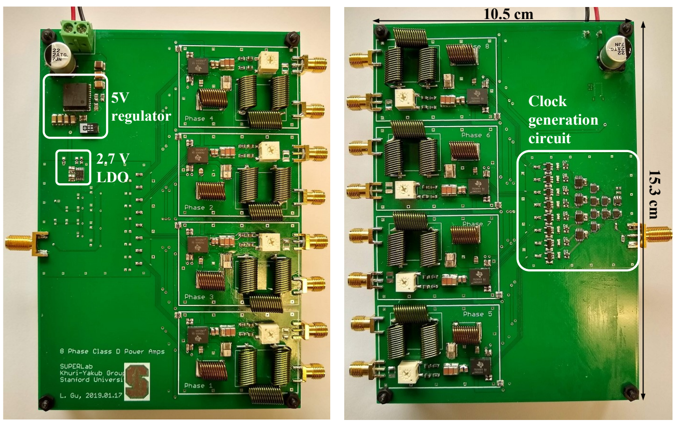

(a) (b)

Fig. 7: 8-phase Class-D GaN RF driver prototype picture. **(a)** Top view, **(b)** Bottom view.

IV. Fast-switching DC Supply

The 2D CMUT array requires different dc bias voltages in the imaging and HIFU modes. In a previous demonstration [4], the transient time of the dc supplies when switching between imaging and HIFU modes was the limiting factor of the ultrasound imaging guided HIFU procedure. With commercial power supplies, the switching transient is 360 ms [4]. We developed the circuit in Fig. 9 that generates the required two dc bias voltages and can quickly switch between them. An LDO regulator was used to generate a stable bias level from a larger input V_{in}. By changing the feedback resistor ratio, we can generate two different output voltages,

$$V_{\text{out}} = \begin{cases} V_{\text{ref}} \frac{R_1+R_2}{R_1}, S_1 \text{ is open,} \\ V_{\text{ref}} \frac{R_1+R_2 \| R_3}{R_1}, S_1 \text{ is short.} \end{cases} \quad (1)$$

When the V_{out} switches from the larger level to the lower one, the charge stored on the output capacitor C_{out} is quickly discharged through the pull-down resistor R_{PD} with a short pulse.

We built a fast-switching dc supply shown in Fig. 10 that has three identical circuits of Fig. 9 to generate the different dc biases required by the system. The LDOs we use here are TPS7A4001 from Texas Instruments. Figure 11 shows that the dc biases generated by the prototype supply switch between different levels for imaging and HIFU operations within 1 ms.

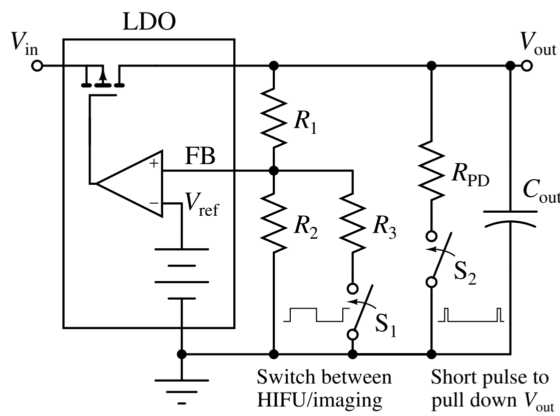

Fig. 9: Fast-switching dc bias circuit.

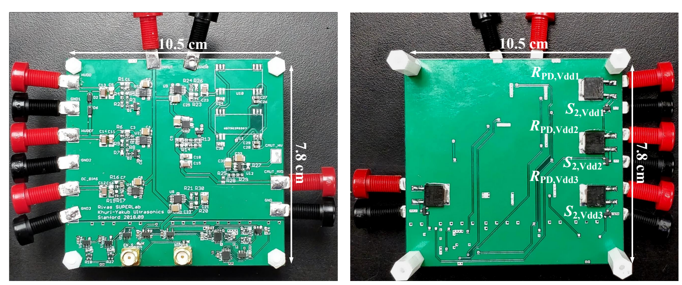

(a) (b)

Fig. 10: Fast-switching dc supply prototype picture. **(a)** Top view, **(b)** Bottom view.

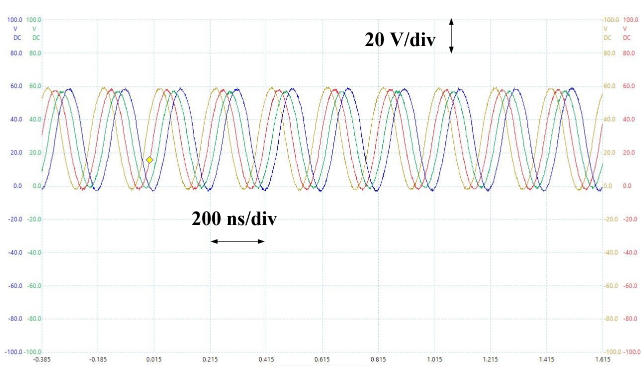

Fig. 8: Measured channel 1-4 RF output with dummy loads.

V. HIFU Testing of 2D CMUT Array

Figure 12 shows the experimental setup to test the 2D CMUT array driven by the newly-developed RF driver for HIFU operation. A 2D CMUT array was mounted on a PGA plugged into a PCB, which was connected to the power electronics. An acrylic tank with vegetable oil was mounted around the PGA and a hydrophone (HGL0200, ONDA Co., U.S.A.) was used to scan the acoustic field.

Figure 13a shows the 2D scan of the acoustic field in XY plane, while the Fig. 13b shows the 2D scan in YZ plane. The

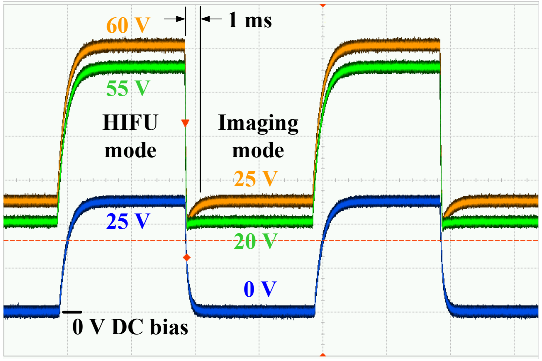

Fig. 11: CMUT DC bias voltages switches between imaging and HIFU mode within 1 ms.

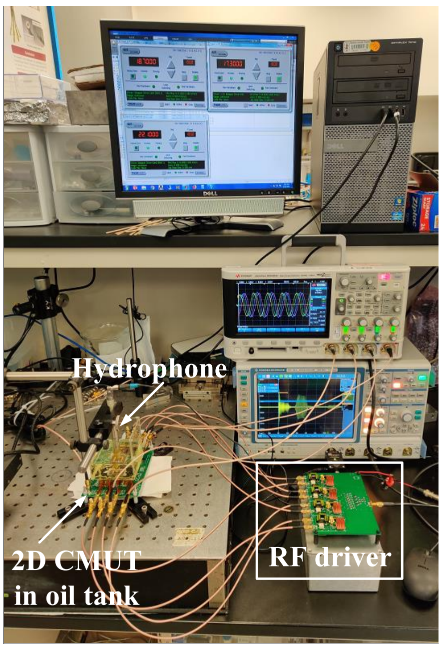

Fig. 12: HIFU testing setup.

transducers produced a focused ultrasound beam when driven by the phased RF amplifiers. The focus size is around 300 μm in the XY plane, as expected, given the depth and the aperture of the CMUT array.

VI. Conclusion

We have designed and implemented compact RF drivers and dc supplies for a 2D CMUT array for HIFU and imaging. Using GaN transistors, we developed a 8-phase switched-mode RF amplifier at 5 MHz that is orders of magnitude smaller than a linear-mode design. We have also developed a simple dc bias circuit that can switch between different voltages within 1 ms in order for the CMUT to alternate between imaging and HIFU operation. This approach could also be used for other dual-mode CMUT array designs. The small size of the RF amplifiers could make it feasible to drive an array with a large number of different phases and to do dynamic electronic focusing in HIFU mode.

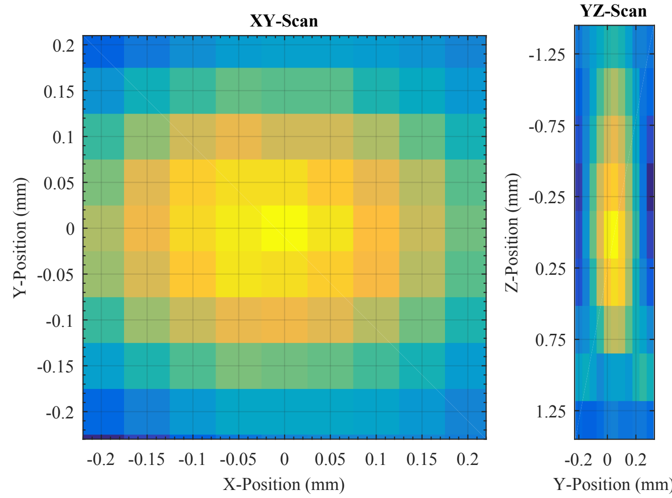

(a) (b)

Fig. 13: 2D focus point scan. **(a)** XY, **(b)** YZ.

Acknowledgment

This work is supported by Cliffdale Technologies. C. N. P. thanks Sao Paulo Research Foundation (FAPESP), grant #2018/00710-1.

References

[1] "State of the Field – Focused Ultrasound," Focused Ultrasound Foundation, Tech. Rep., 2018.

[2] J. H. Jang, M. F. Rasmussen, A. Bhuyan, H. Yoon, A. Moini, C. Chang, R. D. Watkins, J. W. Choe, A. Nikoozadeh, D. Stephens, . Oralkan, K. B. Pauly, and B. Khuri-Yakub, "Dual-mode integrated circuit for imaging and HIFU with 2-D CMUT arrays," in *2015 IEEE International Ultrasonics Symposium (IUS)*, Oct 2015, pp. 1–4.

[3] J. H. Jang, C. Chang, M. F. Rasmussen, A. Moini, K. Brenner, D. N. Stephens, O. Oralkan, and B. Khuri-Yakub, "Integration of a dual-mode catheter for ultrasound image guidance and HIFU ablation using a 2-D CMUT array," in *2017 IEEE International Ultrasonics Symposium (IUS)*, Sept 2017, pp. 1–4.

[4] J. H. Jang, "A dual-mode ultrasound system for imaging and high intensity focused ultrasound (hifu) with a single 2-d capacitive micromachined ultrasonic transducer (cmut) array," Ph.D. dissertation, Stanford University, 2018.

[5] J. J. Macoskey, S. W. Choi, T. L. Hall, E. Vlaisavljevich, J. E. Lundt, F. T. L. Jr, E. Johnsen, C. A. Cain, and Z. Xu, "Using the cavitation collapse time to indicate the extent of histotripsy-induced tissue fractionation," *Physics in Medicine & Biology*, vol. 63, no. 5, p. 055013, 2018.

[6] R. L. Steigerwald, "A comparison of half-bridge resonant converter topologies," *IEEE transactions on Power Electronics*, vol. 3, no. 2, pp. 174–182, 1988.

[7] D. C. Hamill, "Class DE inverters and rectifiers for DC-DC conversion," in *PESC Record. 27th Annual IEEE Power Electronics Specialists Conference*, vol. 1, June 1996, pp. 854–860 vol.1.

[8] W. D. Braun and D. J. Perreault, "A high frequency inverter for variable load operation," *IEEE Journal of Emerging and Selected Topics in Power Electronics*, pp. 1–1, 2019.